Multi-valorisation of giant reed (*Arundo Donax* L.) to give levulinic acid and valuable phenolic antioxidants

Domenico Licursi[1], Claudia Antonetti[1], Marco Mattonai[1], Lorena Pérez-Armada[2], Sandra Rivas[2], Erika Ribechini[1], Anna Maria Raspolli Galletti[1*]

[1] *Department of Chemistry and Industrial Chemistry, University of Pisa, Via G. Moruzzi 13, 56124, Pisa, Italy.*

[2] *Chemical Engineering Department, Polytechnical Building, University of Vigo (Campus Ourense), As Lagoas, 32004, Ourense, Spain.*

*Corresponding author. *E-mail address:* anna.maria.raspolli.galletti@unipi.it

Abstract

Up to now, on the industrial scale, the acid-catalysed hydrothermal conversion of lignocellulosic biomass has been targeted to the production of levulinic acid (LA), while the lignin fate has been neglected, and its use has been limited at most to the energy recovery. Now, an integrated investigation of the hydrothermal process for the synthesis of LA starting from giant reed (*Arundo Donax* L.) was studied taking into account the lignin phenol derivatives present in the liquid phase and in the solid hydrochar. The analysis of the hydrochar was carried out adopting coupled pyrolysis techniques, e.g. Py-GC/MS, TGA/FTIR, and EGA-MS, paying a special attention to the contribution of the evolved simple phenolics. The hydrochar washing fractions were analyzed for the total phenolic content (TPC) and antioxidant activity (AA), adopting TEAC, FRAP, and DPPH standard essays, comparing the antioxidant activities with those deriving from the starting LA-rich mother liquor. Two washing cycles allowed the complete recovery of the phenolic compounds of interest, leached from the porous hydrochar. Also the starting LA-rich liquor was of great interest for the same purpose, having the highest content of these compounds, which must be necessarily removed for the production of the commercial pure LA. Promising antioxidant properties were ascertained for the mother liquor and the hydrochar washings, obtaining good linear correlations between total phenolic compounds (TPC) and antioxidant capacity (TEAC, FRAP, and DPPH). This

multi-valorisation approach contributes to improving the sustainability of the entire LA process and shifts the attention towards the antioxidants, new niche bioproducts of great interest, which add significant economic value to the overall Biorefinery of the lignocellulosic biomass.

Keywords: levulinic acid; lignin; hydrochar; water-soluble phenolics; antioxidants; giant reed.

1. Introduction

The acid-catalyzed hydrothermal route is one of the most promising and environmentally friendly processes for biomass exploitation (Jin et al., 2014). Nowadays, this process is mostly addressed to the production of levulinic acid (LA), the C5 ketocarboxylic acid which is considered as one of the top bio-based platform molecules of greatest industrial interest, thanks to its feasible upgrading into other bio-products, including solvents, plasticizers, fuels and oxygenated fuel additives, monomers for polymers, etc. (Antonetti et al., 2016; Freitas et al., 2016; Pileidis and Titirici, 2016; Rivas et al., 2016). The mature industrial technologies for LA synthesis are based on the exploitation of biomasses rich in C6 or C5 sugars, which are converted through the respective different conversion mechanisms (Van der Waal and De Jong, 2016). Regarding the C6 conversion pathway, LA formation proceeds by acid-catalysed hydrolysis/dehydration, which gives 5-hydroxymethylfurfural (5-HMF) as intermediate (Mukherjee et al., 2015). This furanic compound can be selectively produced, under appropriate reaction conditions (Antonetti et al., 2017a, 2017b), being itself a versatile molecule, which can be further transformed into added-value biofuels and bioproducts. Harsher reaction conditions, in term of acidity, reaction temperature and time, allow the fast transformation of the 5-HMF intermediate into LA, therefore including an additional rehydration step (Antonetti et al., 2016). The technology of the LA process based on the C6 route has been developed by Biofine Renewables (Hayes et al., 2006) and updated by GFBiochemicals (2017), which has recently announced new plans to expand its production on a commercial scale (Silva et al., 2017). During the C6 conversion route, any pentoses of the same lignocellulosic feedstock are converted into furfural (FUR), another very valuable platform chemical (Bernal et al., 2014). This furanic intermediate could be continuously isolated introducing a milder preliminary hydrolysis step (Parton et al., 2013), but actually it is not recovered within the process, remaining in the same reaction medium, where it degrades almost completely, under the harsher reaction conditions suitable for LA synthesis (Antonetti et al., 2015). The main degradation by-products of the

C5/C6 sugar conversion are called “humins”, which derive from condensation reactions involving furanic intermediates (e.g. FUR and 5-HMF from C5 and C6 conversion, respectively) and precursor sugars (e.g. mainly glucose and xylose), with precipitation of an insoluble carbonaceous solid (Heltzel et al., 2016; Tsilomelekis et al., 2016; Wang et al., 2016). Heltzel et al. (2016) have confirmed that the synthesis of huminic by-products involves polymerization of simple furanics, via an aldol addition/condensation pathway. In particular, the authors have studied in depth the thermodynamics of humin formation, suggesting that, taking into account the hydrolysis of C6-sugars, the ring opening of the 5-hydroxymethylfurfural (5-HMF) leads to the main formation of 2,5-dioxo-6-hydroxyhexanal, which undergoes further aldol addition/condensation, resulting, in this way, the primary building block of these furanic by-products. Although not yet unequivocally determined, the humin structure is known to depend on the reaction temperature, time, acid concentration, feedstock structure and its concentration (Zandvoort et al., 2013; Antonetti et al., 2017a). All these parameters must be carefully optimized for the selective synthesis of LA but, unfortunately, humins are always formed under the best LA reaction conditions. In our specific case, starting from C6-sugars, the 5-HMF intermediate is not detected under the best-adopted reaction conditions for LA synthesis, thus highlighting its complete conversion to both LA and humins. About 40 wt% yields of humins were reported in the mineral acid dehydration of aldose, while yields up to 50 wt% of huminic by-products can derive from 5-HMF production (Filiciotto et al., 2017). In addition, humins may derive also from C5 (hemicellulose) degradation reactions, involving furfural formation as the main intermediate, which is no more present, also in this case, under the best reaction conditions for LA synthesis, further confirming its degradation into humins (Licursi et al., 2015). Sumerskii et al. (2010) studied the multi-step humin formation in acidic medium from monosaccharides, underlining that C5-sugars yielded more humins than the C6-ones. This result was ascribed to the higher reactivity of furfural, readily formed from C5 sugars, which undergoes further condensation reactions to humins, whereas lower thermal stability caused the decomposition of 5-HMF into LA and FA. In fact, kinetic studies on humin formation have reported values of activation energies in the range 85-130 kJ mol−1 for humin formation from 5-HMF, whereas lower activation energies were found for the humins formed from furfural (Filiciotto et al., 2017). Regarding the lignin fraction, on the basis of the available optimized LA technology, the isolation of lignin upstream still remains not economically advantageous, adding significant separation costs to the entire LA process. Therefore, lignin is recovered downstream and partially burnt for energy recovery within the same LA plant, otherwise, the remaining stream is currently disposed of. As a consequence, all the new exploitation strategies of lignin fraction recovered after LA production are well-

appreciated, adding further economic value to the entire LA process. Regarding the lignin chemistry during the acid hydrothermal treatment, the combined effect of acidity, temperature and residence time allows the breaking of the more labile ether bonds between its units, leading to its partial fragmentation, but, unfortunately, their fast condensation prevails, resulting in the formation of more stable C-C bonds (Kang et al., 2013; Wang et al., 2013; Zhang et al., 2015). Furthermore, appropriate reaction conditions for lignin dissolution and hydrolysis to monomers by the hydrothermal route are significantly harsher than those adopted for LA synthesis, requiring the use of near-critical or supercritical water (Pavlovič et al., 2013). The native lignin fraction undergoes a degradation, becoming a "*pseudo-lignin*" (Zhuang et al., 2017), which may condense with humins forming the final solid "hydrochar", which is directly separated from the LA-rich mother liquor by simple filtration (Licursi et al., 2017). Thanks to its improved energetic properties, hydrochar can be directly burnt within the same LA plant, thus partially recovering the energy of the entire process but, due to the abundance of this waste stream, which strongly depends on the lignin content of the starting feedstocks, it is necessary to find new exploitation possibilities, thus ensuring the best circular economy approach. In this context, another different exploitation possibility of this hydrochar has been reported by Bernardini et al. (2017), who investigated the synthesis of flexible polyurethane foams by lignin liquefaction in polyolic solvents under microwave irradiation. For different purposes, the entire biomass can be liquefied under relatively mild conditions using polyalcohols, being this step mandatory for subsequent upgrading step, such as its hydrotreatment for the production of oils (Grilc et al., 2014a, 2014b, 2015).

Giant reed (*Arundo Donax* L.) represents a well-known promising feedstock for LA production (Antonetti et al., 2015), due to its rapid growth rate, high resource-use efficiency (of water, radiation, and nutrients), good tolerance to biotic (pests and diseases) and abiotic (heat, freezing, salts) stress and high productivity (Bosco et al., 2016). Furthermore, it represents a very good source of lignin (~20-25 wt%, as Klason lignin), which is composed of *p*-hydroxyphenyl (H), guaiacyl (G), and syringyl (S) phenylpropanoid units, bonded with a predominance of *β*-O-4' aryl ether linkages (~70-80 %), with the remaining part constituted by *β*-*β*', *β*-5', *β*-1', and *α,β*-diaryl ether linkages (You et al., 2013). Gas Chromatography/Mass Spectrometry (GC/MS) technique was adopted to characterize both qualitatively and quantitatively the monosaccharide composition of the starting *Arundo Donax* L., whilst analytical pyrolysis (Py-GC/MS) was used to characterize the starting biomass and the hydrochars recovered after FUR and LA production, thus monitoring the progress of the C5/C6 hydrothermal conversion (Ribechini et al., 2012). It was demonstrated that Py-GC/MS was a powerful tool for monitoring the

chemical modification of the biomass during its catalytic conversion. It was found that, despite the occurred degradation of the lignin, it was still possible to detect simple low-molecular phenols. The solid hydrochar shows a “lignite-like” behavior, which corresponds to very interesting energetic properties (Licursi et al., 2015). Furthermore, this solid waste is rich in carbonyl and hydroxyl reactive functionalities, which make it sustainable for many other applications in environmental, catalysis and polymer chemistry. In particular, a novel green synthesis of flexible polyurethane foams, adopting the *Arundo Donax* L. hydrochar as pseudo-lignin polyol source, has been recently reported (Bernardini et al., 2017).

While the fate of the solid phase deriving from the hydrothermal process has been mostly defined by the characterization activity, little is known about the composition of the phenolic fraction contained in the water phase. This aspect is of paramount importance for closing the Biorefinery of the different hydrothermal processes, thus justifying their complete circular economy (Jin and Enomoto, 2011). For example, Savy et al. (2015a) have investigated the molecular composition of water-soluble lignins obtained after alkaline oxidation treatment of miscanthus (*Miscanthus x Giganteus, Greef et Deuter*) and giant reed (*Arundo Donax* L.). The authors have found that guaiacyl units were the main water-soluble units, followed by syringyl subunits, and few condensed fragments. Low carbohydrate content indicated that alkaline oxidation efficiently separated water-soluble lignin from lignocellulose. In subsequent investigations, the same authors (Savy et al., 2015b, 2016) have proposed the use of these water-soluble lignins as plant biostimulants for the germination and early growth of maize (*Zea mays, L.*) seedlings. Furthermore, the recovery of phenolic compounds from hydrolysates has been mostly investigated after milder pretreatments, as in the case of the pre-hydrolysis of yellow poplar by oxalic acid (Um et al., 2017), whilst, at this state of the art, the opportunity of recovering the phenolic compounds downstream of LA production has not been proposed. In this paper, the study of the lignin behavior during the acid-catalysed hydrothermal conversion of *Arundo Donax* L. to LA has been investigated in-depth, taking into account both solid and liquid phase and the antioxidant activity of the obtained phenolics has been evaluated, thus demonstrating this new exploitation possibility for a multi-valorization of the starting biomass.

2. Materials and methods

2.1. Materials

Giant reed (*Arundo Donax* L.) was provided by the Institute of Life Sciences Scuola Superiore Sant'Anna of Pisa. It came from long-term field trials carried out in Central Italy at the Enrico Avanzi Interdepartmental Centre for Agro-Environmental Research (CIRAA) of the University of Pisa, located in San Piero a Grado (PI) (latitude 43° 68' N, longitude 10° 35' E). The raw biomass was dried at 60 °C in a thermo-ventilated oven until a constant weight was reached and it was stored in a desiccator up to its use. The composition of the whole starting biomass (stalks/leave ratio = 70/30) was the following: 65.3 wt% structural polysaccharides (25.8 wt% hemicellulose and 39.5 wt% cellulose), 26.1 wt% lignin (24.3 wt% as Klason lignin + 1.8 wt% as acid-soluble lignin), 4.2 wt% extractives and 4.4 wt% ash (Licursi et al., 2015).

Hexamethyldisilazane (HMDS) and N,O-bis(trimethylsilyl)trifluoroacetamide (BSTFA) with or without 1% trimethylchlorosilane (TMCS) were purchased from Sigma-Aldrich (Milan, Italy). Tridecanoic acid, hexadecane were purchased from Sigma–Aldrich (USA). All the adopted solvents were HPLC grade.

2.2. Hydrolysis reactions

Hydrolysis reactions were carried out both in the microwave and in autoclave reactors. Regarding the first system, the reactions were carried out by using a commercially available mono-mode microwave reactor (CEM Discover S-Class System, NC, USA), adopting a 35 mL vessel containing a teflon stir bar. This system was equipped with a built-in keypad for programming the reaction procedures and allowing on-the-fly changes. The adopted output power was 300 W, sufficient for rapid heating of the aqueous slurry. Temperature measurement during the reaction was achieved by an IR sensor positioned at the bottom of the cavity, below the vessel. Water and HCl (1.66% wt) were mixed with biomass in a liquid to solid ratio (LSR) of 15 g/g, and introduced into the vessel, then it was closed and irradiated up to the set-point temperature (190 ºC), by employing a fixed ramping time, and maintained at this temperature for 20 minutes. At the end of the reaction, the reactor was rapidly cooled up to room temperature by means of air which was blown directly on the surface of the reactor. The reaction mixture was filtered on a Büchner filter and the mother liquor was analyzed by HPLC for the quantification of the LA and by GC/MS for the identification of phenolic compounds. Instead, the hydrochar was

washed with 50 mL of fresh water, then dried at 105 °C for 24 h and stored in a desiccator up to its next characterization.

Then, the hydrolysis reaction was scaled up in a 1 L Hastelloy C autoclave (Renato Brignole Instruments). The autoclave was equipped with a mechanical magnetic stirrer system, a heating system consisting of three ceramic resistors (each of 500 W) and a thermocouple sensor for monitoring the temperature inside the autoclave. The process control was a Poly Dispersity Index (P.D.I.) and was based on the measurement of the absorbed electrical current by the three resistors. The same solid to liquid weight ratio of the MW tests was adopted. Therefore, water and HCl were mixed with biomass in the same concentration (1.66% wt) and LSR (15 g/g), already adopted for the experiments carried out in microwave (see above). The mixture was introduced into the autoclave and then it was closed and pressurized with 20 bars of nitrogen, heated to the reaction temperature (190 ºC) and maintained at this temperature for 1 h. At the end of each hydrolysis reaction, the autoclave was cooled down to room temperature by means of water, which was flown into the jacket and then degassed. The reaction mixture was recovered and filtered on a Buchner filter, then the mother liquor was analyzed for the identification of the phenolic compounds, for the quantification of LA, total phenolic content and antioxidant activity. Instead, the recovered wet *Arundo Donax* L. hydrochar (~18.5 g) was directly washed on the Büchner filter four times (each time adopting 250 mL of fresh water), dried at 105 °C for 24 h and stored in a desiccator up to its next characterization. Each washing fraction was separately recovered and further characterized for the identification of the phenolic compounds and the determination of the antioxidant activity and the total phenolic content.

2.3. Quantitative analysis of the mother liquor and hydrochar

The quantitative analysis of the mother liquor was performed by High Performance Liquid Chromatography (HPLC). For this purpose, a Perkin Elmer Flexar Isocratic Platform, which was equipped with a differential refractive index detector, was used. 20 µL samples were loaded into a column Benson 2000-0 BP-OA (300 mm × 7.8 mm) kept at 60 °C, employing 0.005 M H_2SO_4 as a mobile phase (flow rate, 0.6 mL min^{-1}). The calibration was carried out using a commercial standard of LA. At least three replicates for each concentration of LA standard were carried out. The reproducibility of the technique was within 2%.

The mass yield of the LA was calculated as follows:

LA mass yield (wt%) = [mass of LA in the reaction mixture (g)/raw material (g)] x 100 (1)

The yield of LA based on theoretical yield was calculated taking into account the stoichiometry of the reaction involving the co-formation of formic acid starting from cellulose.

% on theoretical LA yield = [LA in the reaction mixture (g)/(raw material (g) × cellulose content × 0.7155)] × 100 (2)

Lastly, the mass yield of the recovered hydrochar was calculated as follows:

Hydrochar yield (wt%) = [dried hydrochar (g)/raw material (g)] x 100 (3)

2.4. Pyrolysis-Gas Chromatography/Mass Spectrometry (Py-GC/MS) of the microwave- and autoclave- derived *Arundo Donax* L. hydrochars

Pyrolysis/Gas Chromatography/Mass Spectrometry (Py-GC/MS) was used to investigate the chemical composition of the hydrochars recovered after hydrothermal treatment of *Arundo Donax* L. for LA production, adopting traditional and microwave heating. All the solid samples were dried in an oven at 60 °C for 15 h and milled before the Py-GC/MS analysis. The used ball mill was Mini-Mill PULVERISETTE 23, with grinding bowls (15 mL) and grinding balls (0.5 mm) made of zirconium oxide. Py-GC/MS analysis was carried out using an EGA/PY-3030D Multi-Shot micro-furnace pyrolyser (Frontier Lab, Japan). The pyrolysis temperature was 550°C and interface temperature was 250 °C. Similar amounts (ca. 100 µg) of the sample and HMDS (5 µL) were put into a stainless steel cup and placed into the micro-furnace. The GC injector was used with a split ratio of 1:10 and 280 °C. Chromatographic conditions were as follows: initial temperature 50 °C, 1 min isothermal, 10 °C min^{-1} to 100 °C, 2 min. isothermal, 4 °C min^{-1} to 190 °C, 1 min. isothermal, 30 °C min^{-1} to 280 °C, 30 min. isothermal. Carrier gas: Helium (purity 99.995%), constant flow 1.0 mL min^{-1}. The pyrolyzer was connected to a gas chromatograph 6890 Agilent (USA) equipped with a split/splitless injector, an HP-5MS fused silica capillary column (stationary phase 5% diphenyl- and 95% dimethyl-polysiloxane, 30 m x 0.25 mm i.d., Hewlett Packard, USA) and with a deactivated silica pre-column (2 m x 0.32 mm i.d., Agilent J&W, USA). The GC was coupled

with an Agilent 5973 Mass Selective Detector operating in electron impact mode (EI) at 70 eV. The MS transfer line temperature was 300 °C. The MS ion source temperature was kept at 230 °C and the MS quadrupole temperature at 150 °C. Peak areas of the pyrolysis products were measured, and the data for three replicated analyses averaged and expressed as normalized percentages. The relative standard deviation for the relative areas of the peaks was between 5 and 10%.

2.5. Thermogravimetric analysis/Infrared Spectroscopy (TGA/FTIR) of the microwave- and autoclave-derived *Arundo Donax* L. hydrochars

Thermogravimetric analysis (TGA) was performed by a TGA-DSC 1LF/164 (Mettler Toledo) in high purity N_2 at a flow rate of 60 mL/min. The thermogravimetric balance was coupled with an analyzer FTIR NEXUS (Thermo Fisher Scientific) for the analysis of the evolved volatiles. The sample (~10 mg) was heated from 30 °C up to 900 °C, at a rate of 10 °C min^{-1}, under a nitrogen atmosphere (60 ml min^{-1}). Each FT-IR spectrum was acquired every 32 seconds, resulting in 163 acquired spectra in total, for any experiment. TGA and FTIR were connected by a heated transfer line with a temperature of 220 °C for preventing the condensation of gaseous products. FTIR spectra were acquired in the range 4000-400 cm^{-1}, by using the OMNIC software. Both TG (weight loss as a function of temperature) and DTG (rate of mass loss as a function of the temperature increase) curves were acquired during each experiment. The identification of the FTIR spectra of the hydrochar was carried out on the basis of the available electronic libraries. Each test was carried out in duplicate in order to verify the reproducibility and accuracy of the experimental data.

2.6. Evolved Gas Analysis coupled with Mass Spectrometry (EGA-MS) of the microwave- and autoclave- derived *Arundo Donax* L. hydrochars

Evolved gas analysis-mass spectrometry (EGA-MS) of the starting *Arundo Donax* L. and its hydrochars was carried out using a micro-furnace pyrolyser (Multi-Shot EGA/PY-3030D Pyrolyzer, Frontier Lab) directly coupled with a 5973 Mass Selective Detector (Agilent Technologies, Palo Alto, CA, USA) single quadrupole mass spectrometer *via* a deactivated and uncoated stainless steel transfer tube (UADTM-2.5N, 0.15 mm i.d. × 2.5 m length, Frontier Lab). About 0.2-0.4 mg of sample were adopted for each experiment and placed into a steel sample cup. The temperature of the micro-furnace pyrolyzer was programmed from 50 °C to 700 °C, at a

heating rate of 12 °C min^{-1}, under a helium flow (1 mL min^{-1}), with a split ratio 1:50. The micro-furnace interface temperature was kept at 320 °C and the temperature of the oven was maintained isothermally at 300 °C. The mass spectrometer was operated in EI positive mode (70 eV, scanning m/z 50-600). The MS transfer line temperature was 300 °C. The MS ion source temperature was kept at 230 °C and that of the MS quadrupole at 150 °C.

2.7. Gas Chromatography/Mass Spectrometry (GC/MS) of the mother liquor and hydrochar washings

GC/MS was used to study the composition of the starting liquor derived from *Arundo Donax* L. hydrolysis and hydrochar washings. 1 mL of the starting liquor and each washing were acidified with 1 mL of HCl 6M and then extracted with diethyl ether (600 µL, three times), dried under nitrogen flow and re-dissolved with 1mL of Et_2O. 200 µL of the obtained organic phase were dried under nitrogen flow and derivatized for GC/MS analysis, adding 5 µL of internal standard (tridecanoic acid in acetone) and 20 µL of derivatizing agent N,O-bis(trimethylsilyl)trifluoroacetamide (BSTFA). The reaction took place at 60 °C for 30 minutes in 150 µL of isooctane. 10 µL of the injection internal standard (hexadecane in isooctane) were added before injection in GC/MS (2 µL).

Chromatographic separation was performed with a chemically bonded fused-silica capillary column HP-5MS (Agilent Technologies, Palo Alto, CA, USA), stationary phase 5% phenyl–95% methylpolysiloxane, 0.25 mm internal diameter, 0.25 µm film thickness, 30 m length, connected to 2 m × 0.32 mm internal diameter deactivated fused silica pre-column. The carrier gas was helium (99.995% purity) at a constant flow of 1.2 mL/min. The chromatographic conditions for the separation of silylated compounds were as follows: starting temperature 80 °C, isothermal for 2 min, 10 °C/min. up to 200 °C, 200 °C, isothermal for 3 min, 10 °C min^{-1} up to 280 °C, 280 °C, isothermal for 3 min., 20 °C/min. up to 300 °C, 300 °C, isothermal for 20 min. Chromatograms were recorded in TIC (Total Ion Current, mass range 50–600).

6890N GC system gas chromatograph (Agilent Technologies) coupled with a 5975 mass selective detector (Agilent Technologies) single quadrupole mass spectrometer and equipped with PTV injector, were used. The mass spectrometer was operated in the EI positive mode (70 eV). The MS transfer line temperature was 280 °C, the MS ion source temperature was kept at 230 °C, and the MS quadrupole temperature was kept at 150 °C.

The four fractions recovered from the washing of the autoclave-derived hydrochar were analysed by the same gas chromatographic method. To obtain an estimation of the recovery efficiency, all the chromatographic peaks belonging to identified phenols were integrated and a total chromatogram area was calculated for each fraction. Recovery was then estimated with the formula $R_n = 100 - A_n/A_0$, where R_n is the total recovery after n extractions, A_n is the total area of the n-th chromatogram, and A_0 is the area of the starting liquor.

2.8. Content of soluble compounds in the mother liquor and water soluble fractions recovered from hydrochar washings

The content of soluble compounds (SC) was obtained and expressed on the basis of the content of non-volatile compounds in the liquid phases. The content of non-volatile compounds (NVC) in the autoclave-derived mother liquor and hydrochar washings was measured by oven-drying at 105 ºC until constant weight (Sluiter et al., 2008). The analyses were made in triplicate.

2.9. Total phenolic content (TPC) of the mother liquor and hydrochar washings

TPC of the autoclave-derived mother liquor and hydrochar washings was determined by the Folin-Ciocalteu assay and expressed as gallic acid equivalents (GAE) (Singleton and Rossi, 1965). In addition, water-soluble phenolics were also measured by UV-Vis spectroscopy, as already done for the NREL method, used in our previous work for the characterization of the starting biomass (Licursi et al., 2015).

2.10. Antioxidant activity (AA) of the mother liquor and hydrochar washings

The Trolox Equivalent Antioxidant Capacity (TEAC) assay is based on the scavenging capacity against the ABTS radical (2,20-azinobis-(3-ethyl-benzothiazoline-6-sulfonate)), converting it into a colorless product (Re et al., 1999). The ability to reduce the ferric 2,4,6-tripyridyl-s-triazine (TPTZ) complex under acidic conditions was determined by the FRAP assay (Benzie and Strain, 1996). The scavenging capacity against α,α-diphenyl-β-picrylhydrazyl (DPPH) radical scavenging was determined according to Conde et al. (2008). The inhibition percentage (%IP) of the DPPH radical was calculated as the percent of absorbance reduction after 16 min with respect to the initial value. All the analysis were made in triplicate.

3. Results and discussion

3.1. Synthesis of LA and hydrochar

The *Arundo Donax* L. hydrolysis reactions to give LA and hydrochar were carried out starting from the formulation and the reaction conditions which were previously optimized both in microwave and autoclave systems (Antonetti et al., 2015; Licursi et al., 2015). The optimized results for the synthesis of LA and hydrochar are reported in Table 1, for the two different heating systems:

Table 1, near here

The above data confirm the similarity of the LA and hydrochar mass yields obtained from the two different heating systems. Different reaction times were necessary for achieving a complete conversion of the hexoses, with a theoretical LA yield of ~75-78 %, evaluated respect to the cellulose content of the starting biomass and the stoichiometry of the reaction, in agreement with our previous researches (Antonetti et al., 2015; Licursi et al., 2015). Furthermore, the obtained results highlight that the hydrochar represents the main by-product of the LA synthesis, approaching the mass yield of ~29-30 wt%, evaluated respect to the weight of the starting biomass, and this high yield makes necessary its complementary exploitation. The chemical characterization of the hydrochars synthesized by the two different heating systems is discussed in the next paragraphs.

3.2. Lignin in the solid phase: Py-GC/MS of the microwave- and autoclave- derived *Arundo Donax* L. hydrochars

Table 2 lists the compounds identified in the pyrograms of the hydrochars obtained by microwave- and autoclave- hydrothermal treatment of *Arundo Donax L.* biomass. The identification of the pyrolysis products has been done on the basis of previous works (Mattonai et al., 2016; Ribechini et al., 2012).

Table 2, near here

The data (Table 2 and Fig. S1 in supplementary material) show that the two hydrochars have a similar pattern of the evolved phenolic compounds, thus confirming the similarity between the two hydrolysis reactions. The

pyrolysis products of lignin source include mainly simple phenols, such as guaiacol, methyl guaiacol, ethyl guaiacol, vinyl guaiacol, methyl syringol, vinyl syringol (Wang and Luo, 2017), all with high abundance, deriving from lignin cleavage. On the other hand, Z-coniferyl alcohol, E-coniferyl alcohol, Z-sinapyl alcohol and E-sinapyl alcohol, which were abundant pyrolysis products of the lignin fraction in the starting *Arundo Donax* L., showed low abundance in both hydrochars. This result is related to the performed hydrothermal treatment, which has led to the modification/degradation of the lignin side chains. The most interesting difference in the pyrolysate composition of the two hydrochars regards mainly the presence of oxidized compounds, such as 2-hydroxypropanoic acid (#2), butanedioic acid (#13), vanillin (#26), syringaldehyde (#36), and vanillic acid (#38), which are present in greater percentages in the autoclave-derived hydrochar. This is due to the combined effect of longer reaction time and the difficulty to maintain a totally inert atmosphere in the autoclave reactor. In addition, the pyrolysis products of cellulose and hemicellulose source have not been found, thus demonstrating the complete conversion of the holocellulosic fraction. Finally, it is interesting to note that the evolved aromatic compounds could be advantageously condensed as bio-oil, and therefore their further fractionation and exploitation is highly desired, thus completing the biomass fractionation (Wang and Cheng, 2014).

3.3. Lignin in the solid phase: TGA/FTIR and EGA-MS of the microwave- and autoclave-derived *Arundo Donax* L. hydrochars

Thermal behavior of the microwave- and autoclave- derived *Arundo Donax* L. hydrochars was compared with that of the starting biomass. The thermogravimetric analysis represents a very quick and useful tool for visualizing the changes in chemical composition (cellulose, hemicelluloses and lignin) occurred between the starting biomass and the obtained hydrochar, depending on the employed reaction conditions. In fact, starting *Arundo Donax* L. biomass has its own unmodified cellulose, hemicellulose, and lignin, whilst its derived hydrochars include both degraded lignin and humins.The comparison between the TG/DTG profile of the starting *Arundo Donax* L. biomass and those of the microwave- and autoclave-derived hydrochars is reported in Fig. 1:

Fig. 1, near here

The above figure confirms the analogous thermal profile of both *Arundo Donax* L. hydrochars, but these are very different respect to that of the starting biomass. In detail, DTG curve of the starting biomass shows two intense subsequent degradation steps between 200 and 400 °C, due to the progressive degradation of the hemicellulose and cellulose fractions, respectively. Regarding the thermal behavior of the native lignin, its degradation cannot be significantly appreciated by DTG, being very slow through a wide temperature range (100-800 °C), showing only a weak derivative signal, which falls within those of the carbohydrates (Watkins et al, 2015). Instead, DTG curves of the microwave- and autoclave- derived hydrochars highlight the absence of the thermal degradation steps of hemicellulose/cellulose source, thus revealing the presence of the lignin fraction, which shows a maximum degradation temperature at about 400 °C in both cases. This temperature is higher than that of the native lignin fraction, thus demonstrating the improved thermal stability of the synthesized hydrochars. This is further confirmed by considering the amount of the residual biochar in the TG curves, which is much more higher for both hydrochars rather than for the starting biomass, at each temperature exceeding 500 °C. By coupling TGA with FTIR, the type and distribution of the gaseous products can be linked to the weight loss stages during the hydrochar pyrolysis process. The FTIR identifications of the gaseous compounds deriving from hydrochar pyrolysis at 400 and 850 °C are reported as supplementary materials (Fig. S2 and Fig. S3 in supplementary material), taking into account both the best-matched reference compounds and the available literature data (Yao et al., 2017). Also the Gram-Schmidt plot, which defines the gas emission as a function of the time, is reported as supplementary material in Fig. S4.

3D FTIR spectra of the pyrolysis gaseous products of autoclave-derived hydrochar are reported in Fig. 2, as a clarification of the following discussion:

Fig. 2, near here

FTIR analysis of the gas deriving from hydrochar pyrolysis has revealed the prevailing presence of carbon dioxide and, to a lesser extent, carbon monoxide, both throughout a wide temperature range, e.g. ~150-700 °C and ~300-700 °C, respectively. Furthermore, the presence of methane (~300-800 °C), methanol (~250-550 °C) and acetic acid (~220-750 °C) was also ascertained. Regarding the aromatic compounds, their distinctive absorption bands have not been detected by FTIR, these being minor compounds, not detectable due to the lower sensibility of this technique. In order to get more information about the chemical composition of the

evolved volatiles, with a particular attention to the aromatics, EGA-MS analysis of the same samples was carried out. Thermograms of the gaseous phase evolved during the thermal degradation of the starting *Arundo Donax* L. biomass and its microwave- and autoclave- derived hydrochars are reported in Fig. 3:

Fig. 3, near here

The above thermal profiles retrace mostly those obtained by the traditional TGA analysis (Fig. 1). The EGA-MS profile of the starting *Arundo Donax* L. biomass shows only one main peak at about 330°C. In addition, a shoulder is detected at a higher temperature (380-470°C). The mass spectra highlight that the first step was due to the thermal degradation of both cellulose and lignin, because the relative mass spectrum (Fig. 4, a) contains peaks of carbohydrate (m/z 60, 85, 98, 114,126) and lignin (m/z 137, 167, 180, 194, 208) source (Ribechini et al., 2015; Tamburini et al., 2015). The mass spectra (Fig. 4, b) of the second degradation region (380-470 °C) highlight the presence of the fragments at m/z 77 (benzenes), 91 (alkylbenzenes), 107 (alkylphenols) and 123 (alkylcatechols), among those most abundant. Such peaks are indicative of secondary pyrolysis products due to secondary reactions involving demethylation and demethoxylation of guaiacyl and syringyl units, which occur at high temperatures (Tamburini et al., 2015).

Fig. 4, near here

The *Arundo Donax* L. hydrochars show a very different EGA-MS profile (clearly respect to the starting untreated biomass), both having only one degradation peak between 320 and 540 °C (Fig. 3). This different behavior is due to remarkable differences in chemical composition and thermochemical stability of the analyzed samples. In fact, the acquired data indicate that the hydrochars contain compounds which are more thermally stable, which degrade at higher temperatures than those of the untreated biomass. In addition, the acquired mass spectra within the entire time range (10-43 min, reported in Fig. 5), demonstrate that both hydrochars are pseudo-lignin samples. In detail, the main peaks at m/z 77, 91, 107 and 123, come from lignin pyrolysis reactions to give alkylbenzenes, alkylphenols, and alkylcatechols, involving demethylation and demethoxylation pathways. At the same time, the occurrence of the peaks at m/z 151 and 181, which were produced by all the *p*-substituted

guaiacyl and syringyl units bearing a carbonyl group at the benzylic position, demonstrate that oxidation pathway has occurred during both hydrothermal treatments (Tamburini et al., 2015).

Fig. 5, near here

3.4. Lignin in the liquid phase: GC/MS of the mother liquor and hydrochar washings

The mother liquors which were directly obtained by *Arundo Donax* L. hydrolysis under traditional and microwave heating were further analyzed by GC/MS, in order to evaluate the presence of lignin-source phenols derived from the acid-catalysed hydrothermal treatment of the biomass. Moreover, this analysis is useful for revealing the possible differences caused by these two different heating systems.

GC/MS data (Table 3 and Fig. S5 in supplementary material) highlight the similar pattern of the mother liquors obtained by the two different heating systems. In addition to LA, which represents in both cases the main reaction product, as expected, many simple phenols of typical lignin source have been identified. The comparison between the GC/MS data of the two mother liquors confirms the similarity between their chemical composition, not only regarding the FUR and LA concentrations but also considering the lignin fraction, whose degradation released into the water phase phenolic compounds, which are very similar both for type and amount. The identified phenolics were selected as markers for this investigation and quantified as normalized (%) gas chromatographic areas. Because of the ascertained similarity between the two synthesized hydrochars, only that deriving from traditional heating was employed for the trapped phenols recovery by successive hydrochar washing cycles. Four washing fractions were recovered and analyzed by the same gas chromatographic method, in order to quantify their phenolic compounds, taking as reference those of the mother liquor. It was found that the recovery of water-soluble phenolics from the hydrochar was complete after two washing cycles. Anyway, all the recovered fractions were analyzed for total phenolic content (TPC) and antioxidant activity (AA) together with the starting mother liquor, in order to evaluate the response of the adopted methods and data correlations.

Table 3, near here

3.5. Lignin in the liquid phase: total phenolic content (TPC) and antioxidant activity

First of all, the overall amount of water-soluble phenolics in the mother liquor was estimated by UV-Vis spectroscopy, as measured after NREL hydrolysis procedure (Licursi et al., 2015), resulting 1.4 wt%, evaluated respect to the starting dried biomass. Then, water soluble fractions recovered from hydrochar washings were analyzed for the yield of soluble compounds (SC), the total phenolic content (expressed as gallic acid equivalent "GAE") and the antioxidant activity, evaluated on the basis of different essays, e.g. TEAC or FRAP. Furthermore, the starting mother liquor was analyzed by the same methods, in order to evaluate the effectiveness of phenols removal by subsequent hydrochar washings. The obtained results are reported in Table 4:

Table 4, near here

SC content in the mother liquor was 14.48 g SC/100 g RM, and SC yield increased in 7.1% up to 15.51 g SC/100 g RM with the first washing, and up to 7.5% taking into account a second rinsing. Successive washings diluted and did not improve the soluble solid yield significantly, which resulted in 15.6 g SC/100 g RM.

The mother liquor yielded a TPC of 3.16 g of GAE/100g of *Arundo Donax* L. The first rinsing of treated solids recovered an embedded phenolic fraction being the total phenolic yield raised in 7.1%, reaching up to the amount of 3.38 g GAE/100 g RM. The second rinsing increased this yield up to 8.45%. The successive washings improved the total phenolic yield up to 3.48 g GAE/ 100 g RM.

Conde et al. (2011) have proposed the recovery of antioxidants from selected lignocellulosic wastes subjected to hydrothermal processing (autohydrolysis). The authors reported solid yields of 28.01-11.52 g SC/100 g of corncobs, 15.6-10.1 g SC/100 g of Eucalypt wood or 31.2-10.9 g SC/100 g of almond shells, in the range of 200-240 ºC. The correspondent yields of phenolic compounds were 1.53-2.39 g GAE/100 g of corncobs, 1.31-1.92 g GAE/100 g of Eucalypt wood and 2.06-3.62 g GAE/100 g of almond shells, respectively. Wen et al. (2013) reported that autohydrolysis allowed the solubilization of about 27 g/100 g bamboo culms, and the solubilization of phenolic compounds reached about 3.16 g GAE/100 g RM. This result was higher than those reported by González et al. (2016) starting from autohydrolysis of broom branches (*Cytisus scoparius*). Sipponen et al. (2014) reported that similar phenolic yields in phenolic compounds were obtained from wheat straw during the autohydrolysis pretreatments carried out between 190 and 200 ºC. It is worth to note that in the data obtained in

our work, lower recoveries in SC yielded higher yields in total phenolic compounds, compared to the results reported in the cited literature.

The above data were reprocessed, in order to verify the absence of possible interfering compounds in the analyzed solutions. These data are reported in Fig. 6:

Fig. 6, near here

The above figure highlights a well linear correlation between the TEAC and FRAP values and the concentration of phenolic compounds solubilized in the mother liquor and washing recovered. As expected from its phenolic concentration, the mother liquor showed the best values with 1.13 mmol/L of trolox equivalents and 13.5 mmol/L of ascorbic acid equivalents for TEAC and FRAP assays, respectively. Furthermore, the antioxidant capacities of liquors showed a good correlation between the FRAP values and the TEAC values. A strong correlation between antioxidant capacity and total phenolic content (Folin-Ciocalteu) was also obtained, indicating that phenolic compounds mainly contribute to the antioxidant capacities of these liquors. From the operational standpoint, the third and fourth washings did not provide significant increases in the total soluble recovery and their antioxidant activities. The FRAP value obtained for the *Arundo Donax* L. mother liquor was higher than that obtained for the *Acacia nicolitica* (Rajurkar and Hande, 2011). Al-Laith et al. (2015) reported FRAP values in *Aizoon canariense L.*, *Asphodelus tenuifolius Cav.*, and *Emex spinosus*, falling within the range of the first *Arundo Donax* L. hydrochar washing. Fig. 7 shows the phenolic concentration effect on the DDPH radical scavenging activity, expressed as inhibition percentage (IP%), which represents the amount of DPPH free radical scavenged from its initial concentration by the same assay.

Fig. 7, near here

As expected, the mother liquor and the first washing showed the most active radical scavenger capacities against DPPH radical. It can be observed that the content of phenolics in the extracts is well correlated with their radical scavenger activity. This conclusion suggests that the phenolic compounds which have been independently identified by GC/MS analysis (Table 2) significantly contribute to the overall antioxidant capacity, in agreement with the reported positive correlation between phenolic concentration and antioxidant activity

(Espinoza-Acosta et al., 2016; Turumtay et al., 2014). In particular, lignin degradation, which has occurred during the acid-catalysed hydrothermal treatment, has released simple phenolic compounds, which have been independently identified by GC/MS, such as phenolic alcohols (guaiacol, syringol), as well as phenolic acids (syringic acid, vanillic acid, hydrobenzoic acid) and aldehydes (syringaldehyde), which predominantly contribute to the overall antioxidant activity. These bioactive compounds can be subsequently isolated by different traditional strategies, mainly including solvent extraction, adsorption-desorption, supercritical extraction and membrane processing (Conde et al., 2017; Egües et al., 2012, Moure et al., 2014; Parajó et al., 2008, Um et al., 2017), and research on this topic is in progress.

4. Conclusions

This research has clarified the chemical composition of the simple phenolics of lignin source present in the solid and liquid fractions, obtained after the acid-catalysed hydrothermal treatment of giant reed (*Arundo Donax* L.). Traditional (autoclave) and microwave heating systems were compared, revealing a similarity between the chemical profile of the phenolic compounds in both fractions. The investigation of the solid phase (hydrochar) was carried out by different analytical techniques, Py-GC/MS, TGA/FTIR, and EGA-MS, confirming the possibility of an additional recovery of simple phenolic compounds, deriving from the further thermal degradation of the hydrochar. On the other hand, the liquid fractions, e.g. the mother liquor and the hydrochar washings, were analyzed by GC/MS, identifying many simple phenolic compounds, directly deriving from the acid-catalysed hydrothermal treatment of the starting biomass. Moreover, mother liquor and the water washings were analyzed for the total phenolic content (TPC) and antioxidant activity (AA), adopting TEAC, FRAP, and DPPH standard assays. Promising antioxidant properties were ascertained for the mother liquor and the first two hydrochar washing cycles, obtaining good linear correlations between total phenolic compounds (TPC) and antioxidant capacity (TEAC, FRAP, and DPPH). This new approach can significantly contribute to improving the sustainability of the entire LA process, up to now targeted for the LA production, focusing the attention towards new niche bioproducts, the antioxidants, which surely add significant economic value to the overall Biorefinery of the lignocellulosic biomass.

Acknowledgments

The authors gratefully acknowledge the financial support by the Bank Fundation “Cassa di Risparmio” of Lucca, under “VALCELL” Project. Dr. R. Parton of GFBiochemicals is gratefully acknowledged for helpful discussions.

References

Al-Laith, A.A., Alkhuzai, J., Freije, A., 2015. Assessment of antioxidant activities of three wild medicinal plants from Bahrain. Arabian J. Chem. DOI:10.1016/j.arabjc.2015.03.004.

Antonetti, C., Bonari, E., Licursi, D., Nassi, N., Raspolli Galletti, A.M., 2015. Hydrothermal conversion of giant reed to furfural and levulinic acid: Optimization of the process under microwave irradiation and investigation of distinctive agronomic parameters. Molecules 20, 21232–21253.

Antonetti, C., Licursi, D., Fulignati, S., Valentini, G., Raspolli Galletti, A.M., 2016. New frontiers in the catalytic synthesis of levulinic acid: from sugars to raw and waste biomass as starting feedstock. Catalysts 6, 196-225.

Antonetti, C., Melloni, M., Licursi, D., Fulignati, S., Ribechini, E., Rivas, S., Parajó, J.C., Cavani, F., Raspolli Galletti, A.M., 2017a. Microwave-assisted dehydration of fructose and inulin to HMF catalyzed by niobium and zirconium phosphate catalysts. Appl. Catal., B 206, 364-377.

Antonetti, C., Raspolli Galletti, A.M., Fulignati, S., Licursi, D., 2017b. Amberlyst A-70: A surprisingly active catalyst for the MW-assisted dehydration of fructose and inulin to HMF in water. Catal. Commun. 97, 146-150.

Benzie, I.F.F., Strain, J.J. 1996. The ferric reducing ability of plasma (FRAP) as a measure of ‘‘antioxidant power’’: The FRAP assay. Anal. Biochem. 239, 70–76.

Bernardini, J., Licursi, D., Anguillesi, I., Cinelli, P., Coltelli, M.B., Antonetti, C., Raspolli Galletti, A.M., Lazzeri, A., 2017. Exploitation of *Arundo Donax* L. hydrolysis residue for the green synthesis of flexible polyurethane foams. BioRes. 12, 3630-3655.

Bernal, H.G., Bernazzani, L., Raspolli Galletti, A.M., 2014. Furfural from corn stover hemicelluloses. A mineral acid-free approach. Green Chem. 16, 3734-3740.

Bosco, S., Nassi, N., Roncucci, N., Mazzoncini, M., Bonari, E., 2016. Environmental performances of giant reed (*Arundo Donax L.*) cultivated in fertile and marginal lands: A case study in the Mediterranean. Eur. J. Agron. 78, 20–31.

558 Conde, E., Moure, A., Domínguez, H., Parajó, J.C., 2008. Fractionation of antioxidants from autohydrolysis of
559 barley husks. J. Agric. Food Chem. 56, 10651–10659.
560 Conde, E., Moure, A., Domínguez, H., Parajó, J.C., 2011. Production of antioxidants by non-isothermal
561 autohydrolysis of lignocellulosic wastes. LWT - Food Sci. Technol. 44, 436-442.
562 Conde, E., Moure, A., Domínguez, H., 2017. Recovery of phenols from autohydrolysis liquors of barley husks:
563 kinetic and equilibrium studies. Ind. Crops Prod. 103, 175-184.
564 Egües, I., Sanchez, C., Mondragon, I., Labidi, J., 2012. Antioxidant activity of phenolic compounds obtained by
565 autohydrolysis of corn residues. Ind. Crops Prod. 36, 164-171.
566 Espinoza-Acosta, J.L., Torres-Chávez, P.I., Ramírez-Wong, B., López-Saiz, C.M., Montaño-Leyva, B., 2016.
567 Antioxidant, antimicrobial, and antimutagenic properties of technical lignins and their applications. BioRes.
568 11, 5452-5481.
569 Filiciotto, L., Balu, A.M., Van der Waal, J.C., Luque, R., 2017. Catalytic insights into the production of biomass-
570 derived side products methyl levulinate, furfural and humins. Catal. Today. DOI:
571 10.1016/j.cattod.2017.03.008.
572 Freitas, F.A., Licursi, D., Lachter, E.R., Raspolli Galletti, A.M., Antonetti, C., Brito, T.C., Nascimento, R.S.V.,
573 2016. Heterogeneous catalysis for the ketalization of ethyl levulinate with 1,2- dodecanediol: Opening the
574 way to a new class of bio-degradable surfactants. Catal. Commun. 73, 84-87.
575 Galia, A., Schiavo, B., Antonetti, C., Raspolli Galletti, A.M., Interrante, L., Lessi, M., Scialdone, O., Valenti, M.G.,
576 2015. Autohydrolysis pretreatment of *Arundo donax*: a comparison between microwave-assisted batch and
577 fast heating rate flow-through reaction systems. Biotechnol. Biofuels. 8, 218-235.
578 Garrote, G., Falqué, E., Domínguez, H., Parajó, J.C., 2007. Autohydrolysis of agricultural residues: Study of
579 reaction byproducts. Biores. Technol. 98, 1951-1957.
580 GFBiochemicals, 2017. http://www.gfbiochemicals.com (accessed 1 May, 2017).
581 González, N., Otero, A., Conde, E., Falqué, E., Moure, A., Domínguez, H., 2016. Extraction of phenolics from
582 broom branches using green technologies. J. Chem. Technol. Biotechnol. 92, 1345-1352.
583 Grilc, M., Likozar, B., Levec, J., 2014a. Hydrotreatment of solvolytically liquefied lignocellulosic biomass over
584 NiMo/Al_2O_3 catalyst: Reaction mechanism, hydrodeoxygenation kinetics and mass transfer model based on
585 FTIR. Biomass Bioenergy 63, 300-312.

586 Grilc, M., Likozar, B., Levec, J., 2014b. Hydrodeoxygenation and hydrocracking of solvolysed lignocellulosic
587 biomass by oxide, reduced and sulphide form of NiMo, Ni, Mo and Pd catalysts. Appl. Catal. B. Environ. 150-
588 151, 275-287.
589 Grilc, M., Likozar, B., Levec, J., 2015. Kinetic model of homogeneous lignocellulosic biomass solvolysis
590 inglycerol and imidazolium-based ionic liquids with subsequentheterogeneous hydrodeoxygenation over
591 $NiMo/Al_2O_3$ catalyst. Catal. Today 256, 302-314.
592 Hayes, D.J., Fitzpatrick, S., Hayes, M.H.B., Ross, J.R.H., 2006. The Biofine process – Production of levulinic
593 acid, furfural, and formic acid from lignocellulosic feedstocks, in: Kamm, B., Gruber, P.R., Kamm, M. (Eds,),
594 Biorefineries – Industrial processes and products: status quo and future directions. WILEY-VCH Verlag
595 GmbH, Weinheim, pp. 139-164.
596 Heltzel, J., Patil, S.K.R., Lund, C.R.F., 2016. Humin formation pathways, in: Schlaf, M., Zhang, Z.C. (Eds.),
597 Reaction pathways and mechanisms in thermocatalytic biomass conversion II. Springer, Singapore, pp. 105-
598 118.
599 Jin, F., Enomoto, H., 2011. Rapid and highly selective conversion of biomass into value-added products in
600 hydrothermal conditions: chemistry of acid/base catalyzed and oxidation reactions. Energy Environ. Sci. 4,
601 382–397.
602 Jin, F., Wang, Y., Zeng, X., Shen, Z., Yao, G., 2014. Water under high temperature and pressure conditions and
603 its applications to develop green technologies for biomass conversion, in: Jin, F. (Ed.), Application of
604 hydrothermal reactions to biomass conversion. Springer-Verlag, Berlin, pp. 3-28.
605 Kang, S., Li, X., Fan, J., Chang, J., 2013. Hydrothermal conversion of lignin: A review. Renew. Sust. Energ. Rev.
606 27, 546–558.
607 Licursi, D., Antonetti, C., Bernardini, J., Cinelli, P., Coltelli, M.B., Lazzeri, A., Martinelli, M., Raspolli Galletti, A.M.,
608 2015. Characterization of the *Arundo Donax* L. solid residue from hydrothermal conversion: comparison with
609 technical lignins and application perspectives. Ind. Crops Prod. 76, 1008-1024.
610 Licursi, D., Antonetti, C., Fulignati, S., Vitolo, S., Puccini, M., Ribechini, E., Bernazzani, L., Raspolli Galletti, A.M.,
611 2017. Multivalorisation of waste hazelnut shells: hydrothermal conversion to levulinic acid and production of
612 valuable hydrochar. Bioresour. Technol. 244, 880-888.
613 Mattonai, M., Tamburini, D., Colombini, M.P., Ribechini, E., 2016. Timing in analytical pyrolysis: Py(HMDS)-
614 GC/MS of glucose and cellulose using online micro reaction sampler. Anal. Chem. 88, 9318-9325.

615 Moure, A., Conde, E., Falqué, E., Domínguez, H., Parajó, J.C., 2014. Production of nutraceutics from chestnut
616 burs by hydrolytic treatment. Food Res. Int. 65, 359-366.
617 Mukherjee, A., Dumont, M.-J., Raghavan, V., 2015. Review: Sustainable production of hydroxymethylfurfural and
618 levulinic acid: challenges and opportunities. Biomass Bioenerg. 72, 143-183.
619 Parajó, J.C., Domínguez, H., Moure, A., Díaz-Reinoso, B., Conde, E., Soto, M.L., Conde, M.J., González-López,
620 N., 2008. Recovery of phenolic antioxidants released during hydrolytic treatments of agricultural and forest
621 residues. Electron. J. Environ. Agric. Food Chem. 7, 3243-3249.
622 Parton, R.F.M.J., Rijkers, M.P.W.M., Kroon, J.A., 2013. Continuous production of furfural and levulinic acid.
623 US8426619 B2.
624 Pavlovič, I., Knez, Ž., Škerget, M., 2013. Hydrothermal reactions of agricultural and food processing wastes in
625 sub- and supercritical water: a review of fundamentals, mechanisms, and state of research. J. Agric. Food
626 Chem. 61, 8003–8025.
627 Pileidis, F.D., Titirici, M.M., 2016. Levulinic acid biorefineries: new challenges for efficient utilization of biomass.
628 ChemSusChem 9, 562-582.
629 Rajurkar, N.S., Hande, S.M., 2011. Estimation of phytochemical content and antioxidant activity of some
630 selected traditional Indian medicinal plants. Indian J. Pharm. Sci. 73, 146–151.
631 Re, R., Pellegrini, N., Proteggente, A., Pannala, A., Yang, M., Rice-Evans, C., 1999. Antioxidant activity applying
632 an improved ABTS radical cation decolorization assay. Free Radic. Biol. Med. 26, 1231–1237.
633 Ribechini, E., Zanaboni, M., Raspolli Galletti, A.M., Antonetti, C., Nassi, N., Bonari, E., Colombini, M.P., 2012.
634 Py-GC/MS characterization of a wild and a selected clone of *Arundo Donax*, and of its residues after catalytic
635 hydrothermal conversion to high added-value products. J. Anal. Appl. Pyrol. 94, 223–229.
636 Ribechini, E., Mangani, F., Colombini, M.P., 2015. Chemical investigation of barks from broad-leaved tree
637 species using EGA-MS and GC/MS. J. Anal. Appl. Pyrol. 114, 235-242.
638 Rivas, S., Raspolli-Galletti, A.M., Antonetti, C., Santos, V., Parajó, J.C., 2015. Sustainable production of levulinic
639 acid from the cellulosic fraction of *Pinus Pinaster* wood: Operation in aqueous media under microwave
640 irradiation. J. Wood Chem. Technol. 35, 315-324.
641 Rivas, S., Raspolli-Galletti, A.M., Antonetti, C., Santos, V., Parajó, J.C., 2016. Sustainable conversion of *Pinus*
642 *pinaster* wood into biofuel precursors: A biorefinery approach. Fuel 164, 51-58.

643 Savy, D., Nebbioso, A., Mazzei, P., Drosos, M., Piccolo, A., 2015a, Molecular composition of water-soluble
644 lignins separated from different non-food biomasses. Fuel Process. Technol. 131, 175–181.
645 Savy, D., Cozzolino, V., Vinci, G., Nebbioso, A., Piccolo, A., 2015b. Water-soluble lignins from different
646 bioenergy crops stimulate the early development of maize (*Zea mays* L.). Molecules 20, 19958–19970.
647 Savy, D., Cozzolino, V., Nebbioso, A., Drosos, M., Nuzzo, A., Mazzei, P., Piccolo, A., 2016. Humic-like
648 bioactivity on emergence and early growth of maize (*Zea mays* L.) of water-soluble lignins isolated from
649 biomass for energy. Plant Soil 402, 221–233.
650 Silva, J.F.L., Grekin, R., Mariano, A.P., Filho, R.M., 2017. Making levulinic acid and ethyl levulinate economically
651 viable: a worldwide techno-economic and environmental assessment of possible routes. Energy Technol.
652 DOI: 10.1002/ente.201700594.
653 Singleton, V.L., Rossi, J.A., 1965. Colorimetry of total phenolics with phosphomolybdic-phosphotungstic acid
654 reagents. Am. J. Enol. Vitic. 16, 144–158.
655 Sipponen, M.H., Pihlajaniemi, V., Sipponen, S., Pastinen, O., Laakso, S., 2014. Autohydrolysis and aqueous
656 ammonia extraction of wheat straw: effect of treatment severity on yield and structure of hemicellulose and
657 lignin. RSC Adv. 4, 23177-23184.
658 Sluiter, A., Hames, B., Hyman, D., Payne, C., Ruiz, R., Scarlata, C., Sluiter, J., Templeton, D., Wolfe, J., 2008.
659 Determination of total solids in biomass and total dissolved solids in liquid process samples. Laboratory
660 analytical procedure (LAP). Technical Report NREL/TP-510-42621.
661 Sumerskii, I.V., Krutov, S.M., Zarubin, M.Ya., 2010. Humin-like substances formed under the conditions of
662 industrial hydrolysis of wood. Russ. J. Appl. Chem. 83, 320–327.
663 Tamburini, D., Łucejko, J.J., Ribechini, E., Colombini, M.P., 2015. Snapshots of lignin oxidation and
664 depolymerization in archaeological wood: an EGA-MS study. J. Mass Spectrom. 50, 1103-1113.
665 Tsilomelekis, G., Orella, M.J., Lin, Z., Cheng, Z., Zheng, W., Nikolakis, V., Vlachos, D.G., 2016. Molecular
666 structure, morphology and growth mechanisms and rates of 5-hydroxymethyl furfural (HMF) derived humins.
667 Green Chem. 18, 1983-1993.
668 Turumtay, E.A., İslamoğlu, F., Çavuş, D., Şahin, H., Turumtay, H., Vanholme, B., 2014. Correlation between
669 phenolic compounds and antioxidant activity of Anzer tea (*Thymus praecox* Opiz subsp. *caucasicus* var.
670 *caucasicus*). Ind. Crops Prod. 52, 687-694.

671 Um, M., Shin, G.-J., Lee, J.-W., 2017. Extraction of total phenolic compounds from yellow poplar hydrolysate and
672 evaluation of their antioxidant activities. Ind. Crops Prod. 97, 574-581.
673 Van der Waal, J.C., De Jong, E., 2016. Avantium chemicals: The high potential for the levulinic product tree, in:
674 de María, P.D. (Ed.), Industrial biorenewables: a practical viewpoint. John Wiley & Sons, Hoboken, pp. 97-
675 120.
676 Van Zandvoort, I., Wang, Y., Rasrendra, C.B., van Eck, E.R.H., Bruijnincx, P.C.A., Heeres, H.J., Weckhuysen,
677 B.M., 2013. Formation, molecular structure, and morphology of humins in biomass conversion: influence of
678 feedstock and processing conditions, ChemSusChem 6, 1745–1758.
679 Wang, L., Cheng, D., 2014. Biomass pyrolysis and bio-oil utilization, in: Wang, L. (Ed.), Sustainable Energy
680 Production. CRC Press, Taylor & Francis Group, Boca Raton, Chapter 18, pp. 361-378.
681 Wang, S., Lin, H., Zhao, Y., Chen, J., Zhou, J., 2016. Structural characterization and pyrolysis behavior of humin
682 by-products from the acid-catalysed conversion of C6 and C5 carbohydrates. J. Anal. Appl. Pyrol. 118, 259-
683 266.
684 Wang, S., Luo, Z., 2017. Pyrolysis of lignin, in: Wang, S., Luo, Z. (Eds.), Pyrolysis of biomass. Walter de Gruyter
685 GmbH, Berlin, pp. 103-140.
686 Wang, H., Tucker, M., Ji, Y., 2013. Recent development in chemical depolymerization of lignin: A review. J. Appl.
687 Chem. DOI: 10.1155/2013/838645.
688 Watkins, D., Nuruddin, M., Hosur, M., Tcherbi-Narteh, A., Jeelani, S., 2015. Extraction and characterization of
689 lignin from different biomass resources. J. Mater. Res. Technol. 4, 26-32.
690 Wen, J.-L., Sun, S.-N., Yuan, T.-Q., Xu, F., Sun, R.-C., 2013. Fractionation of bamboo culms by autohydrolysis,
691 organosolv delignification and extended delignification: Understanding the fundamental chemistry of the lignin
692 during the integrated process. Bioresour. Technol. 150, 278–286.
693 Yao, Z., Ma, X., Wu, Z., Yao, T., 2017. TGA–FTIR analysis of co-pyrolysis characteristics of hydrochar and
694 paper sludge. J. Anal. Appl. Pyrol. 123, 40-48.
695 You, T.-T., Mao, J.-Z., Yuan, T.-Q., Wen, J.-L., Xu, F., 2013. Structural elucidation of the lignins from stems and
696 foliage of *Arundo Donax* Linn.. J. Agric. Food Chem. 61, 5361–5370.
697 Zhang, L., Yan, L., Wang, Z., Laskar, D.D., Swita, M.S., Cort, J.R., Yang, B., 2015. Characterization of lignin
698 derived from water-only and dilute acid flowthrough pretreatment of poplar wood at elevated temperatures.
699 Biotechnol. Biofuels DOI: 10.1186/s13068-015-0377-x.

Zhuang, J., Wang, X., Xu, J., Wang, Z., Qin, M., 2017. Formation and deposition of pseudo-lignin on liquid hot-water-treated wood during the cooling process. Wood Sci. Technol. 51, 165–174.

Table 1 LA and hydrochar mass data yield obtained from the optimized Arundo Donax L. hydrolysis reactions, carried out in microwave and autoclave reactors at 190 °C.

Heating system	Time (min.)	LA mass yield (wt%)	% on theoretical LA yield	Hydrochar mass yield (wt%)
Microwave	20	21.3	75.4	28.9
Autoclave	60	22.1	78.2	29.7

745 **Table 2** Identification of the pyrolysis products for the microwave- and autoclave- derived *Arundo Donax* L.
746 hydrochars, under the best reaction conditions for LA synthesis. N° refers to the peak numeration reported in
747 Fig. 1.

N°	Name	Microwave (%)	Autoclave (%)	Source
1	Phenol (TMS)	2.9	2.8	
2	2-Hydroxypropanoic acid (2TMS)	2.0	10.0	
3	2-Hydroxyacetic acid (2TMS)	0.5	1.1	
4	Guaiacol	0.3	0.0	G
5	*o*-Cresol (TMS)	0.5	0.7	
6	Levulinic acid (TMS)	16.7	15.4	
7	*m*-Cresol (TMS)	4.2	0.3	
8	Methyl-guaiacol	0.2	0.0	G
9	1,2-Dihydroxybenzene (TMS)	0.6	0.2	
10	Guaiacol (TMS)	6.5	4.9	G
11	Hydroxyxylene (TMS)	3.4	2.3	
12	Phosphate (3TMS)*	---	---	
13	Butanedioic acid (2 TMS)	4.1	12.8	
14	1,2-Dihydroxybenzene (2TMS)	1.2	0.0	
15	4-Methylguaiacol (TMS)	13.0	0.5	G
16	2-Methyl-3-hydroxy-(4H)-pyran-4-one (TMS)	0.1	0.0	
17	1,4-Dihydroxybenzene (2TMS)	0.1	0.0	
18	4-Methylcatechol (2TMS)	1.5	1.8	G
19	4-Ethylguaiacol (TMS)	2.9	1.5	G
20	Syringol (TMS)	4.0	3.7	G
21	4-Vinylguaiacol (TMS)	5.3	6.4	G
22	4-Ethylcatechol (2TMS)	0.3	0.3	G
23	Eugenol (TMS)	0.3	0.6	G
24	4-Methylsyringol (TMS)	7.7	6.1	G
25	E-Isoeugenol (TMS)	0.1	0.2	G
26	Vanillin (TMS)	1.1	2.8	G
27	1,2,3-Trihydroxybenzene (3TMS)	0.3	0.0	
28	5-Methyl-3-methoxy-1,2-benzenediol (2TMS)	1.9	1.7	
29	4-Ethylsyringol (TMS)	0.7	0.4	S
30	Z-Isoeugenol (TMS)	1.3	1.9	G
31	4-Vinylsyringol (TMS)	1.9	2.5	S
32	1,2,4-Trihydroxybenzene (3TMS)	0.8	0.5	
33	Acetovanillone (TMS)	1.1	0.8	G
34	4-Hydroxy benzoic acid (2TMS)	0.2	0.4	
35	4-Hydroxy-3,5-dimethoxy cinnamic acid methyl ester (TMS)	0.3	0.3	S
36	Syringaldehyde (TMS)	1.1	2.2	S
37	E-Propenylsyringol (TMS)	0.8	1.2	S

38	Vanillic acid (2TMS)	3.7	4.7	G
39	Acetosyringone (TMS)	1.1	1.3	S
40	Z-Coniferyl alcohol (2TMS)	0.2	0.3	G
41	Syringic acid (2TMS)	1.8	2.7	S
42	E-Coniferyl alcohol(2 TMS)	2.0	2.4	G
43	Syringylpropanol (2TMS)	0.1	0.5	S
44	3,4-Dihydroxy cinnamyl alcohol (3TMS)	0.0	0.1	G
45	Palmitic acid (TMS) *	---	---	
46	E-Synapyl alcohol (2TMS)	1.2	1.7	S
47	E-2-Methoxy-3,4-dihydroxy cinnamic alcohol (3TMS)	0.1	0.1	G
48	Stearic acid (TMS) *	---	---	

Note a: “G” refers to the pyrolysis products deriving from coniferyl lignin units, and “S” to those from syringyl ones.

Table 3 Compounds identified (by GC/MS) in the mother liquors recovered after *Arundo Donax* L. hydrolysis in microwave and autoclave systems, under the best reaction conditions. N° refers to the numbers of the peaks which are correspondingly reported in Figure 7.

N°	Compound	m/z
1	Levulinic acid 2TMS	188, 173, 155, 145, 131, 129, 99, 75
2	Unknown I	202, 187, 160, 143, 129, 112, 75
3	1,2-dihydroxybenzene TMS	182, 167, 166, 151, 136, 91, 75
4	Unknown II	202, 187, 173, 159, 145, 131, 75, 73
5	Guaiacol TMS	196, 181, 166, 151, 136
6	3-hydroxy-6-methyl-(2H)-pyran-2-one TMS	198, 183, 111, 73
7	(E/Z)-2,4-dihydroxypent-2-enal 2TMS	260, 245, 217, 147, 143, 73
8	(E/Z)-2,4-dihydroxypent-2-enal 2TMS	260, 245, 217, 147, 143, 73
9	2,4-dihydroxypentanal 2TMS	262, 247, 147, 129, 73
10	1,2-dihydroxybenzene 2TMS	254, 239, 166, 151, 136, 73
11	Propanedioic acid 2TMS	276, 261, 232, 217, 204, 186, 147, 73
12	Unknown III	276, 261, 233, 190, 171, 159, 147, 133, 103, 73
13	3-hydroxy-2-hexenoic acid 2TMS	274, 259, 230, 215, 147, 75, 73
14	1,4-dihydroxybenzene 2TMS	254, 239
15	Syringol TMS	226, 211, 196, 151, 153, 73
16	3-hydroxyacetophenone TMS	208, 193, 165, 151, 135, 123, 105, 91, 73
17	2,3-dihydroxycyclopent-2-enone 2TMS	258, 243, 73
18	4-hydroxyacetophenone TMS	208, 193, 151, 135, 89, 73
19	3-methoxy-1,2-benzenediol 2TMS	284, 269, 254, 239, 153, 73
20	Unknown IV	222, 207, 179, 163, 149
21	Butylated hydroxytoluene	220, 205, 177, 145, 105, 91, 57
22	Vanillin TMS	224, 209, 194, 179, 163
23	Unknown V	240, 225, 196, 181, 165, 150, 73
24	3-hydroxybenzoic acid 2TMS	282, 267, 223, 193, 149, 91, 73
25	Unknown VI	243, 240, 225, 216, 215, 198, 197, 183, 173, 129, 126, 123, 113, 111, 109, 95, 85, 75, 73, 55
26	Acetovanillone TMS	238, 223, 208, 193, 73
27	4-hydroxybenzoic acid 2TMS	282, 267, 223, 207, 193, 73
28	3-(3-methoxy-4-hydroxyphenyl)propanal TMS	252, 237, 222, 209, 193, 179, 163, 149, 73
29	Syringaldehyde TMS	254, 239, 224, 153
30	Tridecanoic acid TMS (IS)	289, 271, 145, 129, 117, 75, 73
31	Vanillic acid 2TMS	312, 297, 282, 267, 253, 223, 207, 193, 179, 165, 126, 73
32	Acetosyringone TMS	268, 253, 238, 223, 208, 193, 165, 137, 119, 104
33	3-(3,5-dimethoxy-4-hydroxyphenyl)propanal TMS	282, 267, 252, 239, 209, 179, 166, 151
34	Unknown VII	370, 355, 311, 267, 223, 193, 165, 137
35	Unknown VIII	384, 369, 267, 173, 147, 125, 73
36	3-(3-methoxy-4,5-dihydroxyphenyl)propanal 2TMS	340, 325, 297, 267, 209, 73
37	Syringic acid 2TMS	342, 327, 312, 297, 283, 253, 223, 141, 73
38	Unknown IX	366, 321, 291, 251, 218, 203, 176, 161, 147, 73

39	3,4-dhydroxy-5-methoxybenzoic acid 3TMS	400, 385, 341, 311, 297, 253, 237, 223, 195, 73
40	Unknown X	338, 323, 249, 233, 193, 73
41	Unknown XI	364, 349, 292, 278, 263, 207
42	Unknown XII	276, 261, 219, 203, 73
43	Unknown XIII	366, 351, 193, 173, 73
44	Unknown XIV	426, 411, 396, 381, 223, 193, 173, 73
45	Unknown XV	384, 369, 294, 251, 222, 193, 177, 149, 135, 121, 73

795 **Table 4** Soluble compounds, total phenolic content, and antioxidant activity (on basis of TEAC and FRAP
796 assays) per g of raw biomass, for the mother liquor and hydrochar washings.

	Soluble Compounds	Total Phenolic Content	TEAC	FRAP
	mg SC/ g RM	mg GAE/g RM	mg trolox/g RM	mg AAE / g RM
Mother liquor	145±1	31.6±0.6	0.212±0.009	35.9±0.7
1st Washing	10.3±0.2	2.23±0.06	0.053±0.003	2.52±0.05
2nd Washing	0.723±0.078	0.442±0.005	0.068±0.003	0.547±0.014
3rd Washing	0.231±0.025	0.278±0.005	0.023±0.002	0.352±0.015
4th Washing	0.225±0.036	0.290±0.005	0.024±0.000	0.375±0.013
Liquor+1st Washing	155	33.8	0.265	38.4
Liquor+1st and 2nd Washings	156	34.2	0.332	38.9
Total sum	156	34.8	0.379	39.7

797 RM: Raw Material (biomass). SC: Soluble Compounds. GAE: Gallic Acid Equivalent. AAE: Ascorbic Acid
798 Equivalent.
799
800
801
802
803
804
805
806
807
808
809
810
811
812
813
814

Figure captions

Fig. 1 TG and DTG curves of the starting *Arundo Donax* L. and microwave- and autoclave- derived hydrochars, the latter produced under the optimized reaction conditions to give LA.

Fig. 2 3D FTIR spectra of the gas evolved from the autoclave-derived *Arundo Donax* L. hydrochar.

Fig. 3 Thermograms of the gas evolved from the starting *Arundo Donax* L. and its microwave- and autoclave-derived hydrochars, the latter synthesized under the optimized reaction conditions to give LA.

Fig. 4 Mass spectra of the starting *Arundo Donax* L. biomass obtained by EGA-MS: a) integration time: 10-27 min. and b) 27-43 min.

Fig. 5 Mass spectra of the a) microwave- and b) autoclave- derived *Arundo Donax* L. hydrochar obtained by EGA-MS (integration time: 10-43 min).

Fig. 6 Correlation between the concentration of phenolic compounds (expressed as mg GAE/L) and the antioxidant activity assayed by TEAC and FRAP.

Fig. 7 Correlation between the total phenolic compounds and the DPPH radical scavenging activity in the mother liquor and hydrochar washings.

844

Figure 1

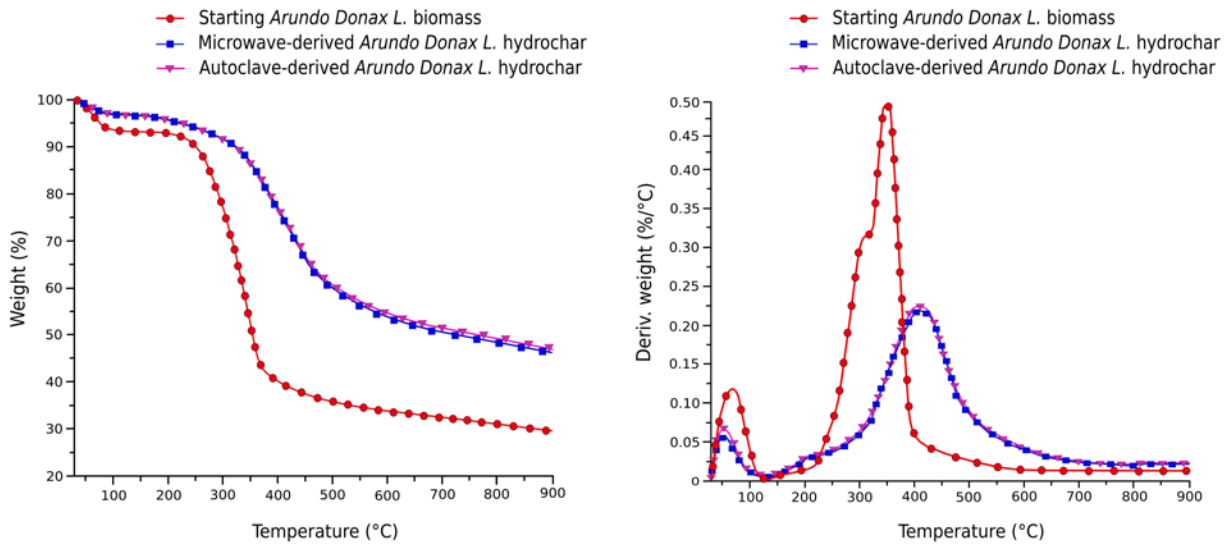

845

846

847

848

Figure 2

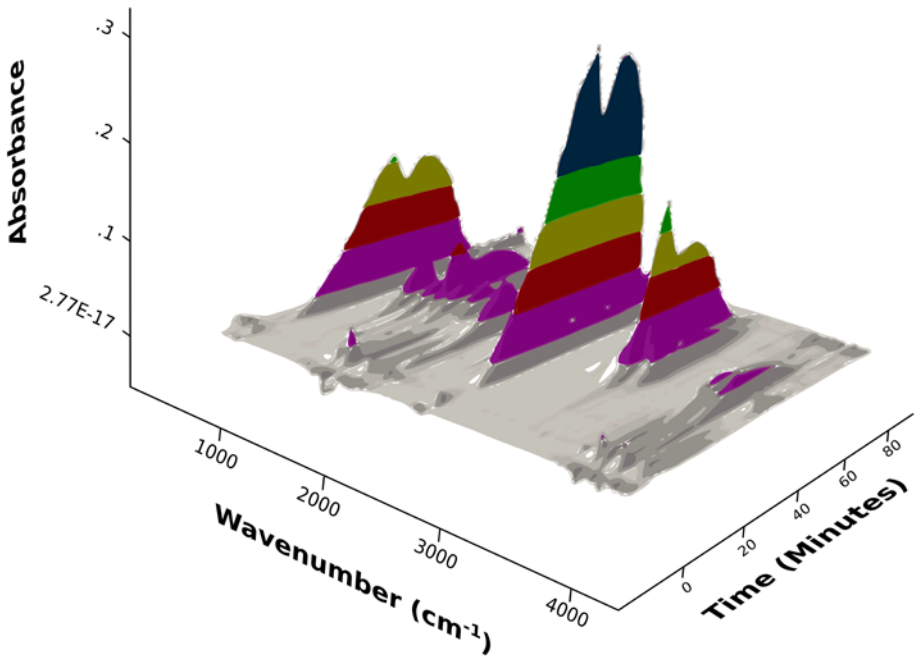

849

850

851

852

853

Figure 3

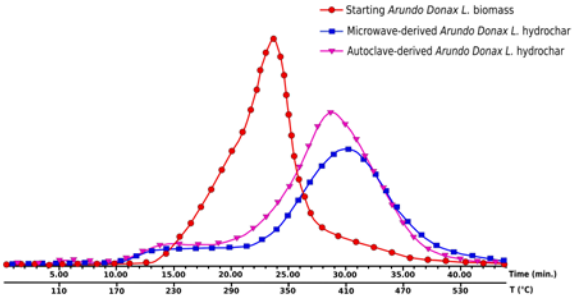

Figure 4

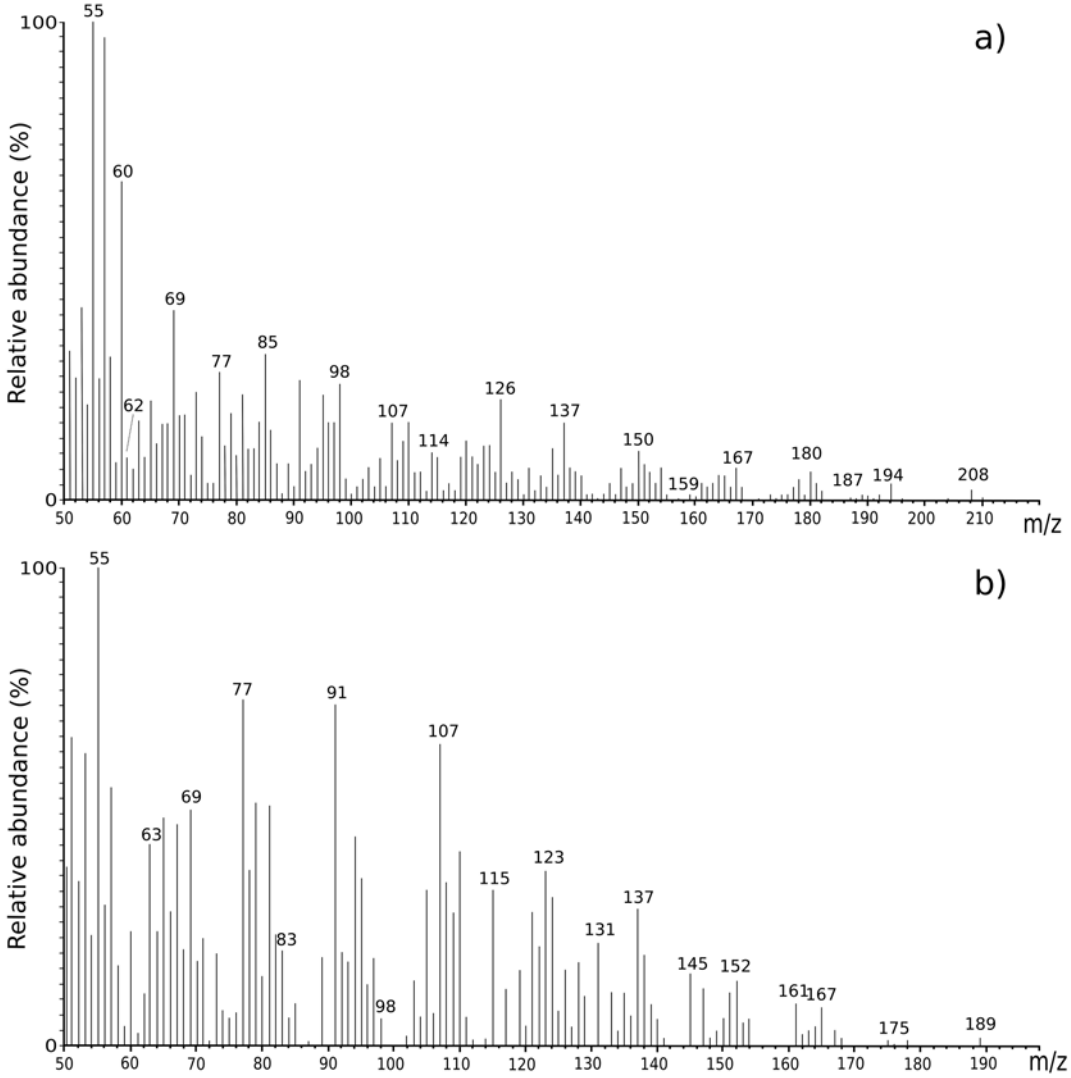

Figure 5

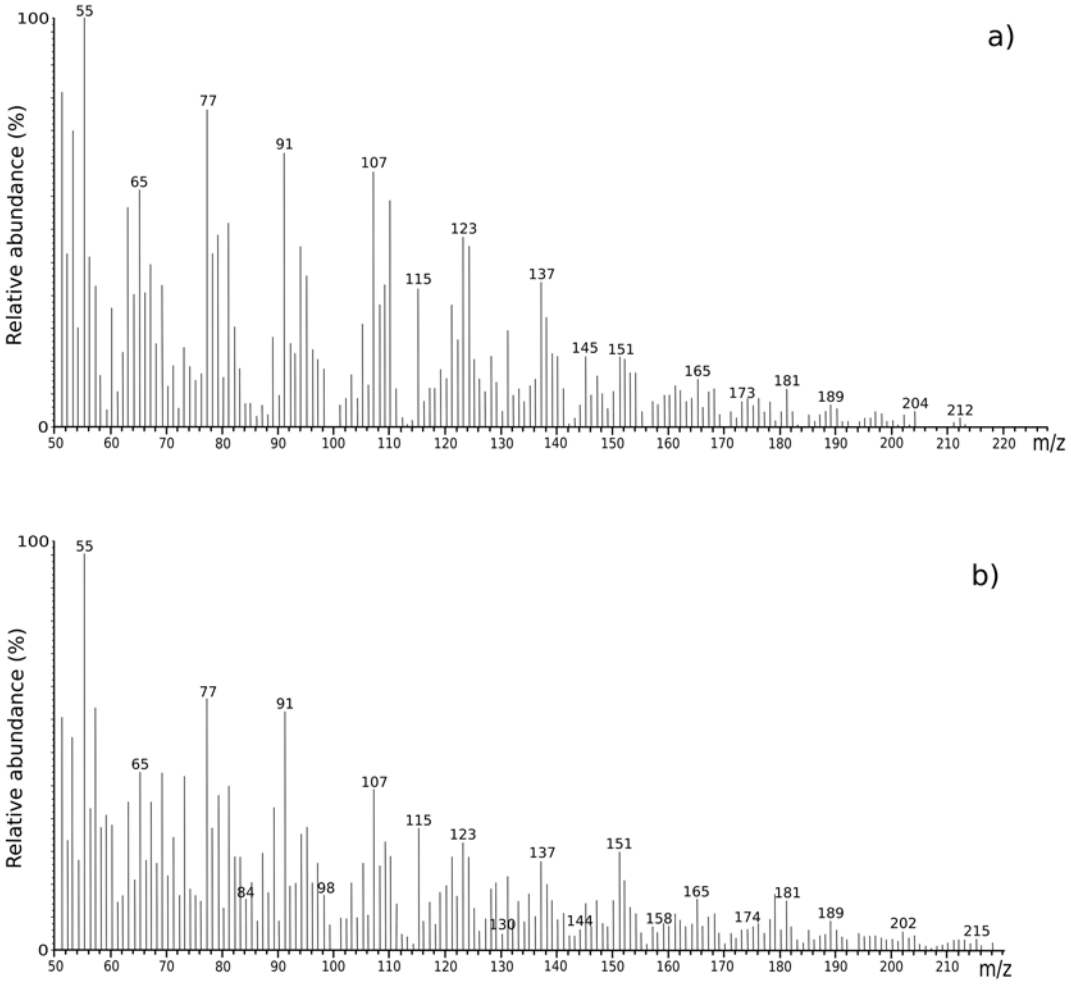

Figure 6

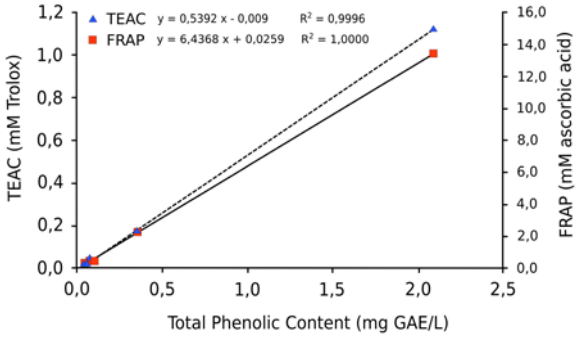

870

Figure 7

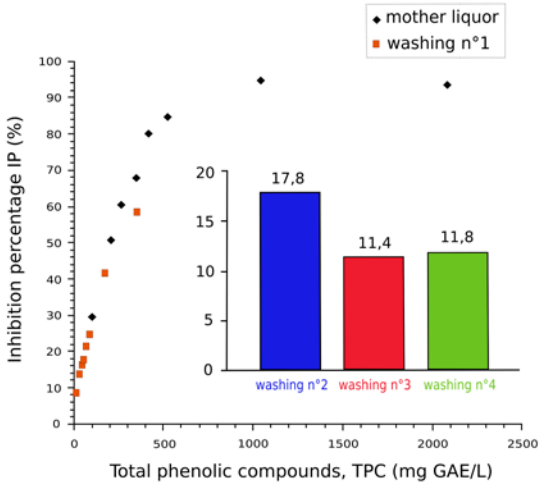

871

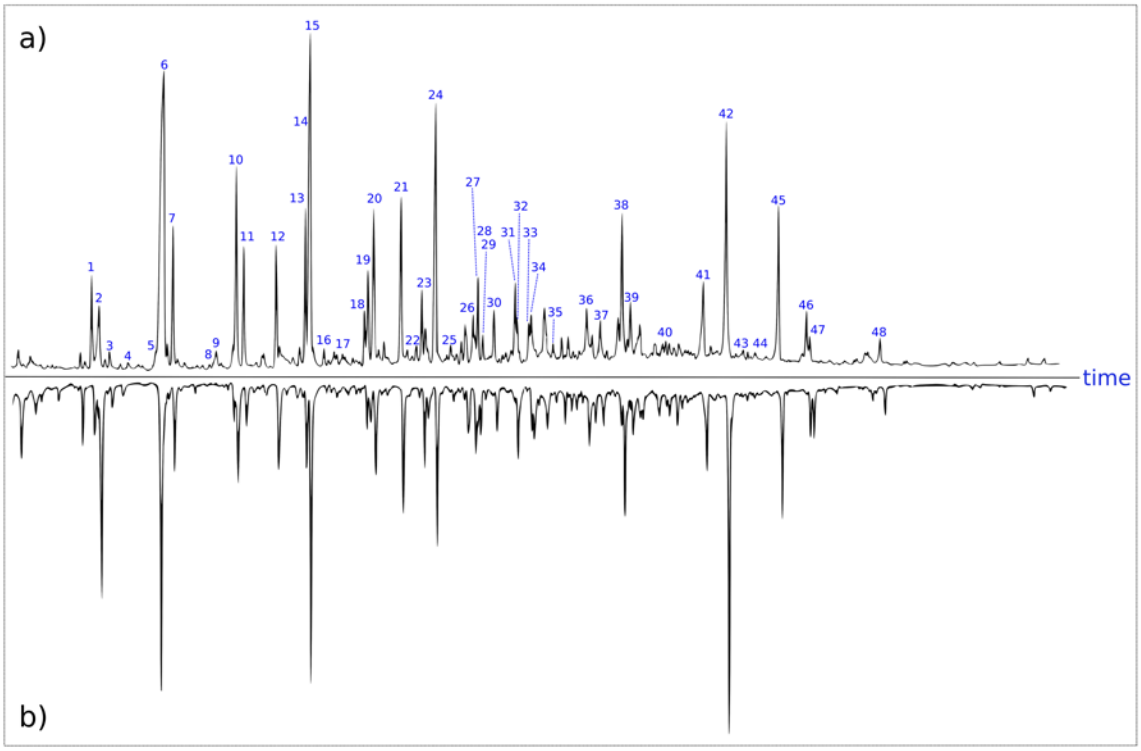

Fig. S1 Pyrograms of **(a)** microwave- and **(b)** autoclave- derived *Arundo Donax* L. hydrochars, under the best reaction conditions for LA synthesis. The identification of the numbered peaks is reported in Table 2.

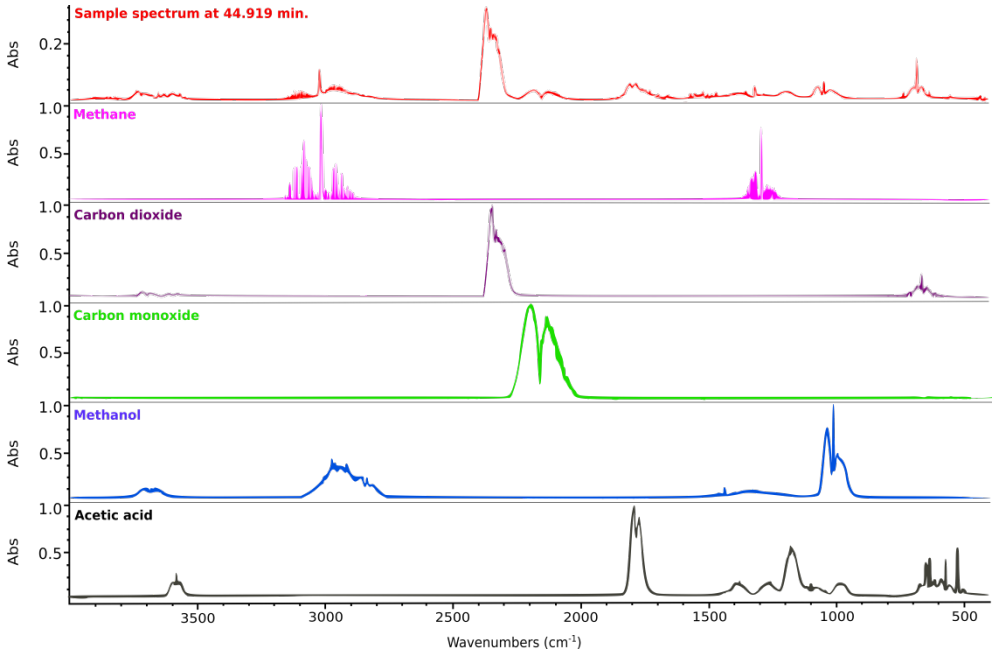

Fig. S2 Comparison of the FTIR spectrum of the gas deriving from autoclave- derived hydrochar pyrolysis in TGA at 400 °C and those of the best-matched compounds, on the basis of the available electronic libraries.

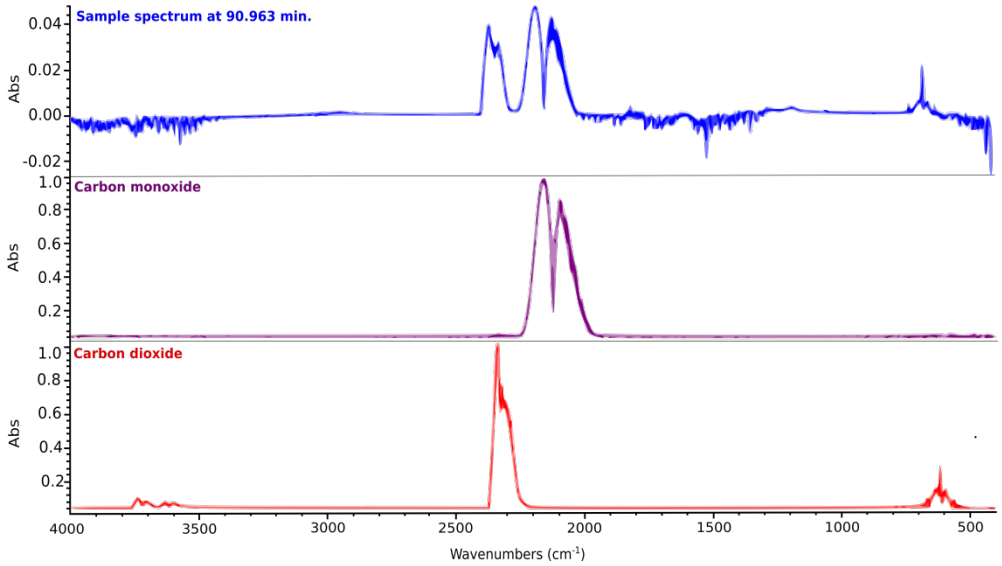

Fig. S3 Comparison of the FTIR spectrum of the gas deriving from autoclave- derived hydrochar pyrolysis in TGA at 850 °C and those of the best-matched compounds, on the basis of the available electronic libraries.

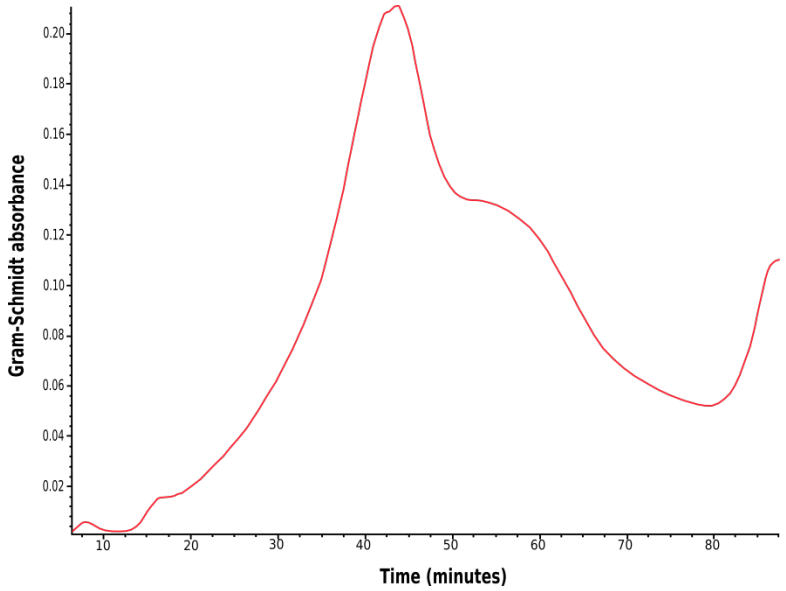

Fig. S4 Gram-Schmidt plot of the gas evolved from the autoclave-derived *Arundo Donax* L. hydrochar.

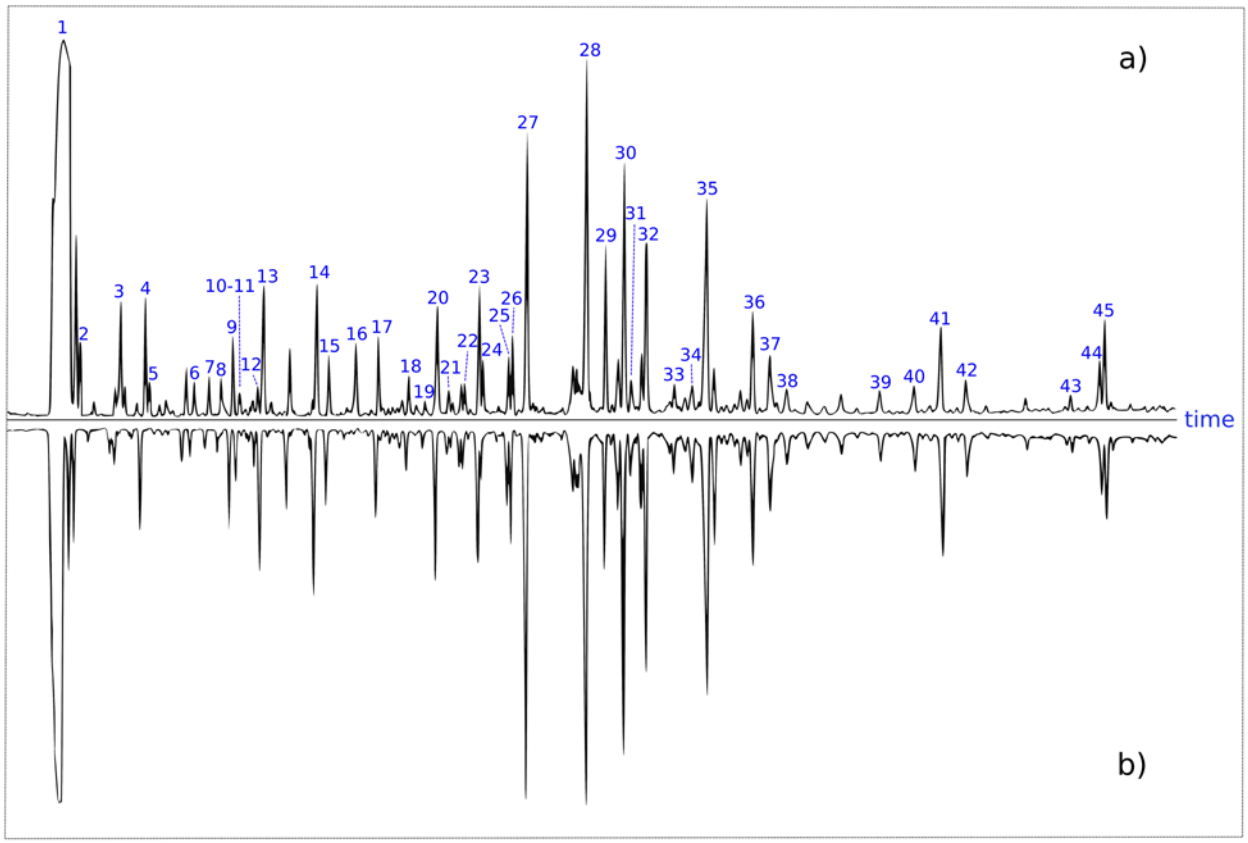

Fig. S5 GC/MS chromatograms of the mother liquors recovered after *Arundo Donax* L. hydrolysis in **(a)** microwave and **(b)** autoclave systems, under the best reaction conditions to give LA. The corresponding assignments are reported in Table 3.